

Gigantic enhancement of spin Seebeck effect by phonon drag

Hiroto Adachi^{1,2,1,a)} Ken-ichi Uchida^{3,1} Eiji Saitoh^{3,1,2,4,1} Jun-ichiro Ohe^{1,2,1} Saburo Takahashi^{3,2,1} and Sadamichi Maekawa^{1,21}

¹ Advanced Science Research Center, Japan Atomic Energy Agency, Tokai 319-1195, Japan

² CREST, Japan Science and Technology Agency, Sanbancho, Tokyo 102-0075, Japan

³ Institute for Materials Research, Tohoku University, Sendai 980-8755, Japan

⁴ PRESTO, Japan Science and Technology Agency, Sanbancho, Tokyo 102-0075, Japan

(Dated: 28 September 2018)

We investigate both theoretically and experimentally a gigantic enhancement of the spin Seebeck effect in a prototypical magnet $\text{LaY}_2\text{Fe}_5\text{O}_{12}$ at low temperatures. Our theoretical analysis sheds light on the important role of phonons; the spin Seebeck effect is enormously enhanced by nonequilibrium phonons that drag the low-lying spin excitations. We further argue that this scenario gives a clue to understand the observation of the spin Seebeck effect that is unaccompanied by a global spin current, and predict that the substrate condition affects the observed signal.

When a temperature gradient is applied to a ferromagnet, a force is induced acting on electrons' spin to drive spin currents. This phenomenon termed the spin Seebeck effect (SSE)¹⁻³ has recently drawn tremendous attention as a new source of spin currents needed for future spin-based electronics.^{4,5} SSE is now established as an universal aspect of ferromagnetic materials as it has been observed in a variety of materials ranging from a metallic ferromagnet¹ $\text{Ni}_{81}\text{Fe}_{19}$ and a semiconducting ferromagnet² GaMnAs to an insulating magnet³ $\text{LaY}_2\text{Fe}_5\text{O}_{12}$. Besides its impact on the technological application, SSE offers a number of new topics on the interplay of heat and spin currents,^{6,7} and it triggered the emergence of the new field named "spin caloritronics"⁸ in the rapidly-growing spintronics community.

A mystery concerning SSE was how conduction electrons can sustain the spin voltage over so long range of several millimeters in spite of the short conduction electrons' spin-flip diffusion length λ_{sf} , which is typically of several tens nanometers. This problem has recently been resolved by a series of experiments on spin currents using magnetic insulators. A recent experiment on the electric signal transmission through a magnetic insulator⁹ highlights the role of the low-lying magnetic excitation of localized spins, i.e., magnons, by demonstrating that magnons transmit the spin current over a long distance of several millimeters. A subsequent experiment on SSE for a magnetic insulator³ $\text{LaY}_2\text{Fe}_5\text{O}_{12}$ confirmed that the magnon-based scenario can explain the SSE experiment at room temperature, since the length scale associated with magnons $\gg \lambda_{\text{sf}}$. However, a new issue on SSE was brought by a very recent experiment on a ferromagnetic semiconductor² GaMnAs , where it was demonstrated, by cutting the magnetic coupling in GaMnAs while keeping the thermal contact, that SSE can be observed even

in the absence of global spin current flowing through GaMnAs . Obviously, the scenario of magnon-mediated SSE^{10,11} fails to explain the experiment, showing that the full understanding of SSE has not yet been reached.

For a deep understanding of the physics behind SSE, we here explore the low-temperature behavior of SSE in an insulating magnet $\text{LaY}_2\text{Fe}_5\text{O}_{12}$. Figure 1 shows a schematic illustration of our device structure.¹² An in-plane external magnetic field \mathbf{H} and a uniform temperature gradient ∇T were applied along the z direction [see FIG. 1 (a)]. The ∇T generates a spin voltage across the $\text{LaY}_2\text{Fe}_5\text{O}_{12}/\text{Pt}$ interface, and injects (ejects) a spin current I_s into (from) the Pt wire, and in the Pt wire, a part of the injected/ejected I_s is converted into a charge voltage through the so-called inverse spin-Hall effect (ISHE):¹³

$$V_{\text{ISHE}} = \Theta_H(|e|I_s)(\rho/w), \quad (1)$$

where $|e|$, Θ_H , ρ and w are the absolute value of electron

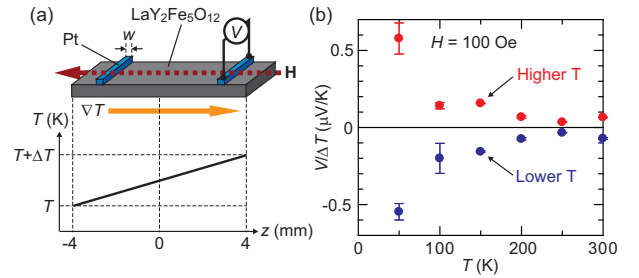


FIG. 1. (Color online) Gigantic enhancement of SSE in $\text{LaY}_2\text{Fe}_5\text{O}_{12}$ at low temperatures. (a) Schematic illustration of the $\text{LaY}_2\text{Fe}_5\text{O}_{12}/\text{Pt}$ sample and the temperature profile along the z direction. Here \mathbf{H} denotes an external magnetic field (with magnitude H). The sample comprises a $\text{LaY}_2\text{Fe}_5\text{O}_{12}$ film with $8 \times 4 \text{ mm}^2$ rectangular shape and two separated Pt wires with the width w attached to the $\text{LaY}_2\text{Fe}_5\text{O}_{12}$ surface at the interval of 5.6 mm. (b) T dependence of $V/\Delta T$ at $H = 100 \text{ Oe}$.

^{a)}hiroto.adachi@gmail.com

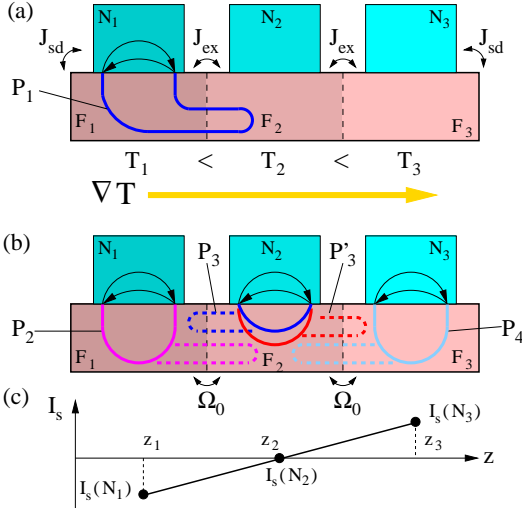


FIG. 2. (Color online) Diagrammatic representation of the thermal spin injection process. (a) Magnon-mediated SSE. Here the system is composed of ferromagnet (F , in the experiment $\text{LaY}_2\text{Fe}_5\text{O}_{12}$) and nonmagnetic metals (N , in the experiment Pt), which are divided into three temperature domains of F_1/N_1 , F_2/N_2 , and F_3/N_3 with their local temperatures of T_1 , T_2 , and T_3 . The thin solid lines with arrows (bold lines without arrows) are electron (magnon) propagators. Here, J_{sd} (J_{ex}) is the strength of the s - d coupling at the F/N interface (the exchange coupling in F). (b) Phonon-dragged SSE where the dashed lines are phonon propagators. The process P_4 injects the spin current with the same magnitude as (but opposite sign to) the process P_2 due to the relation $T_1 - T_2 = -(T_3 - T_2)$, while no spin current is injected into N_2 because of the cancellation between the two relevant processes P_3 and P_3' . Here, $\Omega_0 = \sqrt{K_{ph}/M_{ion}}$ with the ion mass M_{ion} and the elastic constant K_{ph} in F . (c) Calculated spatial dependence of the spin current injected into N_i ($i = 1, 2, 3$).

charge, spin-Hall angle, resistivity and width of the Pt wire, respectively. Therefore, the ∇T -driven spin injection, or SSE, is electrically detectable. In FIG. 1 (b), we show the temperature (T) dependence of $V_{\text{ISHE}}/\Delta T$ at $H = 100$ Oe, measured when the Pt wires are attached to the lower- and higher-temperature ends of the $\text{LaY}_2\text{Fe}_5\text{O}_{12}$ layer, respectively. The sign of $V/\Delta T$ is reversed between these Pt wires, a situation consistent with SSE-induced ISHE. Notable is that, at $T = 50$ K, the magnitude of $V/\Delta T$ is dramatically enhanced.

A simple scenario of the magnon-mediated SSE^{10,11} [FIG. 2 (a)] is unable to explain the observed low- T enhancement. If such a scenario could explain the experiment, the low- T enhancement of V_{ISHE} would come from either the enhancement of the spin-Hall angle Θ_H or that of the magnon lifetime; otherwise I_s due to magnon-mediated SSE is a monotonic increasing function of T as discussed below. From the T -dependence of the spin-Hall conductivity,¹⁴ we conclude that there is no enhancement of Θ_H at low T . While the possibility of the enhance-

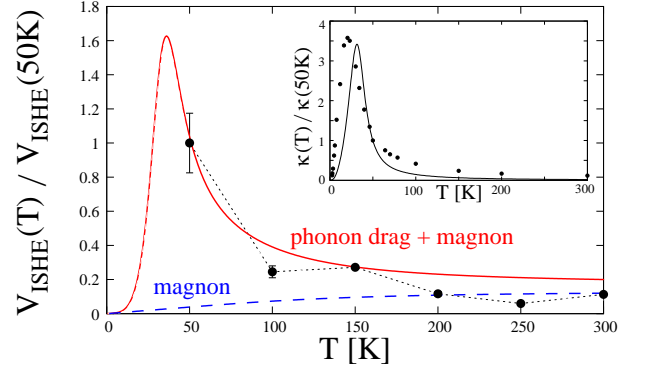


FIG. 3. (Color online) Comparison of experimental and theoretical SSE signal. Solid circles: experimental spin Seebeck data for $\text{LaY}_2\text{Fe}_5\text{O}_{12}$ (Dotted line is a guide to the eye). The solid curve: calculated T -dependence of V_{ISHE} due to the sum of the phonon-dragged SSE and the magnon-mediated SSE. The dashed curve: calculated T -dependence of V_{ISHE} due only to the magnon-mediated SSE. We have assumed T -independent Θ_H and α , and used $T_D = 565$ K²³ and $T_M = 560$ K. The data are normalized by its value at 50 K except that the result for magnon-mediated SSE is plotted to reproduce the room-temperature signal. Inset: experimental thermal conductivity κ for $\text{Y}_3\text{Fe}_5\text{O}_{12}$ taken from Ref. 23 (solid circles) and the result of the fit (solid curve) using Eq. (4).

ment of magnon lifetime is not conclusively excluded, judging from the ferromagnetic resonance linewidth in $\text{Y}_3\text{Fe}_5\text{O}_{12}$ ¹⁵ as a measure of the inverse magnon lifetime, it does not seem to be the case. Therefore, we need a new mechanism to account for the observed low- T enhancement of SSE.

Here, the gigantic enhancement of SSE for $\text{LaY}_2\text{Fe}_5\text{O}_{12}$ below room temperature is analyzed in the light of phonon-drag mechanism.^{16–18} Back in 1946 in the context of thermoelectrics, Gurevich pointed out¹⁶ that the thermopower can be generated by a stream of phonons driven by the temperature gradient, which then drag electrons and cause their convection. This idea, known nowadays as phonon-drag mechanism, has been established^{17,18} as a principal mechanism causing the low- T enhancement¹⁹ of the thermopower. Because SSE is a spin counterpart of the Seebeck effect, it is natural to expect that a similar physics underlies SSE. It is this approach that we adopt in the present work.

Our theoretical analysis starts from considering the model shown in FIG. 2 (a). The key point in our model is that the temperature gradient ∇T is applied over the ferromagnet, but there is locally no temperature difference between the ferromagnet (F) and the attached nonmagnetic metals (N). We assume that each temperature domain is initially in local thermal equilibrium, then we switch on the interactions among the domains and calculate the nonequilibrium dynamics of spin density in N .

The central quantity that characterizes SSE is the spin current I_s injected into N (in experiment Pt), since it

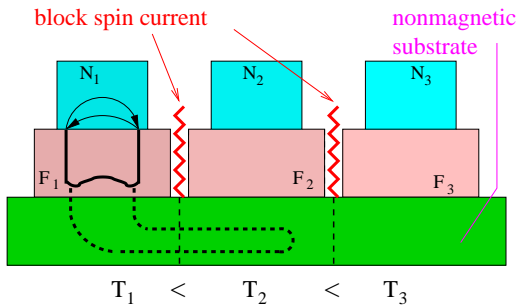


FIG. 4. (Color online) Schematic illustration of SSE unaccompanied by a global spin current. The phonon-drag process which explains the experiment² is shown. The meaning of each line (propagator) is the same as in FIG. 2.

is proportional to the experimentally-detectable electric voltage via ISHE [Eq. (1)]. Following Ref. 11, the spin current $I_s^{\text{mag}}(N_1)$ injected into N_1 due to the magnon-mediated SSE^{10,11} is calculated as

$$I_s^{\text{mag}}(N_1)/\Delta T = \left(\frac{P}{\alpha}\right) \int_0^{T_M/T} ds \frac{(T/T_M) s^2}{4 \sinh^2(s/2)}, \quad (2)$$

where α is the Gilbert damping constant, T_M is the characteristic temperature corresponding to the magnon high-energy cutoff, and P is a nearly-temperature-independent coefficient.²⁰ Equation (2) means that the magnon-mediated SSE cannot explain the low- T enhancement of the signal (the dashed curve in FIG. 3).

Now we proceed to a detailed analysis of the T -dependence of SSE in terms of the phonon-drag mechanism. The Feynman diagram for the phonon-drag process in the present situation is shown in FIG. 2 (b), where the phonons feel the temperature difference between F_1 and F_2 , and drag magnons through the magnon-phonon interaction. Since the nonequilibrium phonons affect the magnon dynamics, this process injects spin current into N_1 . The important point is that the spin current I_s^{drag} injected in this process becomes proportional to the phonon lifetime τ_{ph} as¹²

$$I_s^{\text{drag}}(N_1)/\Delta T = P' \tau_{\text{ph}} \mathcal{B}_1 \mathcal{B}_2, \quad (3)$$

where $\mathcal{B}_1 = \frac{(T/T_D)^5}{4\pi^3} \int_0^{T_D/T} du \frac{u^6}{\sinh^2(u/2)}$ and $\mathcal{B}_2 = \frac{(T/T_M)^{9/2}}{4\pi^2} \left(\frac{k_B T_M \tau_{\text{sf}}}{\hbar}\right)^3 \int_0^{T_M/T} dv \frac{v^{7/2}}{\tanh(v/2)}$ with the Debye temperature T_D , and P' is a nearly-temperature-independent coefficient.²² Since τ_{ph} in a high-purity specimen is known to increase steeply at low T because of the rapid suppression of umklapp scattering,²¹ it leads to the drastic enhancement of the phonon-dragged SSE. In our analysis, the T -dependence of τ_{ph} is extracted from the thermal conductivity data for $\text{Y}_3\text{Fe}_5\text{O}_{12}$ ²³ (see the inset of FIG. 3) using^{21,24}

$$\kappa(T) = (1/3)v_{\text{ph}}^2 C_{\text{ph}}(T)\tau_{\text{ph}}(T), \quad (4)$$

where v_{ph} is the phonon velocity, and $C_{\text{ph}}(T) = 9N_D k_B (T/T_D)^3 \int_0^{T_D/T} dw \frac{w^3}{4 \sinh^2(w/2)}$ is the phonon specific heat with the number of phonon modes N_D . After getting the information on $\tau_{\text{ph}}(T)$, we calculate the T -dependence of V_{ISHE} resulting from the phonon-dragged SSE. The result, plotted in FIG. 3 (the solid curve), shows an excellent description of the low- T enhancement of SSE.²⁵ Our analysis demonstrates that the phonon-drag mechanism is of crucial importance to understand SSE below the room temperature.

Finally, we show in FIG. 4 our interpretation on the observation of SSE that is unaccompanied by a global spin current,² where the heat is carried by phonons through the nonmagnetic substrate while the spin is injected locally at the F/N interface. This interpretation is reinforced when we recall that the magnitude of the spin Seebeck signal is enhanced with decreasing T even well below the Curie temperature, whose tendency is consistent with the phonon-drag mechanism as is seen in FIG. 3. Furthermore, the fact that the experiment was done below the room temperature supports the the phonon-drag-based scenario, since the phonon-drag process becomes more effective at low T as emphasized in the previous paragraph. All these considerations strongly support that the SSE experiment for GaMnAs can be interpreted in terms of the phonon-drag mechanism, and results in a prediction that the substrate condition affects the observed signal. Our demonstration opens a new route to control spin currents by means of phonons and stimulates further progresses in spin caloritronics.

This work was supported by a Grant-in-Aid for Scientific Research in Priority Area 'Creation and control of spin current' (19048009, 19048028), a Grant-in-Aid for Scientific Research A (21244058), the Global COE for the 'Materials Integration International Centre of Education and Research', a Grant-in-Aid for Young Scientists (No. 22740210) all from MEXT, Japan, a Grant for Industrial Technology Research from NEDO, Japan, Fundamental Research Grants from CREST-JST, PRESTO-JST, TRF, and TUIAREO, Japan.

- ¹K. Uchida, S. Takahashi, K. Harii, J. Ieda, W. Koshibae, K. Ando, S. Maekawa, and E. Saitoh, *Nature* **455**, 778 (2008).
- ²C. M. Jaworski, J. Yang, S. Mack, D. D. Awschalom, J. P. Heremans, and R. C. Myers, *Nature Mater.* **9**, 898 (2010).
- ³K. Uchida, J. Xiao, H. Adachi, J. Ohe, S. Takahashi, J. Ieda, T. Ota, Y. Kajiwara, H. Umezawa, H. Kawai, G. E. W. Bauer, S. Maekawa, and E. Saitoh, *Nature Mater.* **9**, 894 (2010).
- ⁴I. Žutić, J. Fabian, and S. D. Sarma, *Rev. Mod. Phys.* **76**, 323 (2004).
- ⁵Maekawa, S. (ed) *Concepts in Spin Electronics* (Oxford Univ. Press, Oxford, U.K., 2006).
- ⁶J. C. Slonczewski, *Phys. Rev. B* **82**, 054403 (2010).
- ⁷A. Slachter, F. L. Bakker, J-P. Adam, and B. J. van Wees, *Nature Phys.* **6**, 879 (2010).
- ⁸Spin Caloritronics, edited by G. E. W. Bauer, A. H. MacDonald, and S. Maekawa, special issue of *Solid State Commun.*, **150**, 459 (2010).
- ⁹Y. Kajiwara, K. Harii, S. Takahashi, J. Ohe, K. Uchida, M. Mizuguchi, H. Umezawa, H. Kawai, K. Ando, K. Takanashi, S. Maekawa, and E. Saitoh, *Nature* **464**, 262 (2010).

- ¹⁰J. Xiao, G. E. W. Bauer, K. Uchida, E. Saitoh, and S. Maekawa, Phys. Rev. B **81**, 214418 (2010).
- ¹¹H. Adachi, J. Ohe, S. Takahashi, and S. Maekawa, Phys. Rev. B (in press); arXiv:1010.2325.
- ¹²See supplemental material for experimental and theoretical details.
- ¹³E. Saitoh, M. Ueda, H. Miyajima, and G. Tatara, Appl. Phys. Lett. **88**, 182509 (2006).
- ¹⁴L. Vila, T. Kimura, and Y. Otani, Phys. Rev. Lett. **99**, 226604 (2007).
- ¹⁵C. Vittoria, P. Lubitz, P. Hansen, and W. Tolksdorf, J. Appl. Phys. **57**, 3699 (1985).
- ¹⁶L. Gurevich, Zh. Eksp. Teor. Fiz. **16**, 193 (1946).
- ¹⁷F. J. Blatt, P. A. Schroeder, C. L. Foiles, and D. Greig, *Thermoelectric Power of Metals* (Plenum Press, New York, 1976).
- ¹⁸E. M. Lifshitz and L. P. Pitaevskii, *Physical Kinetics* (Pergamon, New York, 1982).
- ¹⁹H. P. R. Frederikse, Phys. Rev. **92**, 248 (1953); C. Herring, *ibid.* **96**, 1163 (1954); T. H. Geballe and G. W. Hull, *ibid.* **94**, 1134 (1954).
- ²⁰ $P = (k_B \tau_{sf} / 8\pi^5 \hbar^3) \times L$ with $L = 0.1 \times N_{\text{int}} (J_{sd}^2 S_0) \chi_N (a / \lambda_{sf})^3 (a_S / \Lambda)$, where N_{int} and J_{sd} are the number of localized spins and the strength of the s - d exchange coupling at the N_1 - F_1 interface; χ_N , τ_{sf} , and λ_{sf} are the paramagnetic susceptibility, the spin relaxation time, and the spin diffusion length in N_1 ; Λ and a_S are the dimension and lattice constant of the effective block spin of F_1 .
- ²¹N. W. Ashcroft and N. D. Mermin, *Solid State Physics* (Saunders College, Philadelphia, 1976).
- ²² $P' = 0.5 \times \tilde{g}^2 k_B T_D L / (\pi^2 M_{\text{ion}} v_{\text{ph}}^2 \hbar^3)$ with the dimensionless magnon-phonon coupling constant \tilde{g} and the ion mass M_{ion} .
- ²³G. A. Slack and D. W. Oliver, Phys. Rev. B **4**, 592 (1971).
- ²⁴For the T -dependence of τ_{ph} , we introduce a model $\tau_{\text{ph}}(T) / \tau_{\text{ph}}(T=0) = [1 + \frac{1}{a_0} e^{-b_0(T_D/T)}]^{-1} [1 + \frac{1}{c_0}(T/T_D)]^{-1}$ with fit parameters $(a_0, b_0, c_0) = (2 \times 10^{-4}, 0.55, 0.01)$, where the first term represents the low- T enhancement (ref. 21) $\tau_{\text{ph}} \sim e^{b_0 T_D/T}$ originating from the steep suppression of the umklapp scattering at $T \sim b_0 T_D$, while the second term captures the high- T behavior (ref. 21) $\tau_{\text{ph}} \sim 1/T$.
- ²⁵Note that theoretically the signal due to the phonon-dragged SSE has a close-to-linear spatial dependence [see FIG. 2 (c)] as is observed in experiments, the reason of which is obvious from FIG. 2 (b). In addition, the length scale associated with the phonon-dragged SSE is set by that related to the energy conservation, such that it can be as long as several millimeters.

SUPPLEMENTAL MATERIAL

1. Experimental details

The single-crystal $\text{LaY}_2\text{Fe}_5\text{O}_{12}$ (111) film with the thickness of $3.9 \mu\text{m}$ was grown on a $\text{Gd}_3\text{Ga}_5\text{O}_{12}$ (111) substrate by liquid phase epitaxy. The 15-nm-thick Pt wires were then sputtered in an Ar atmosphere. The length and width of each Pt wire are 4 mm and 0.1 mm, respectively. The temperatures of the lower- and higher-temperature ends of the sample were respectively stabilized to T and $T + \Delta T$, where T was controlled in the range of 300-50 K by means of a closed-cycle helium refrigerator.

2. Derivation of Eq. (3)

Following Ref. [S1], the spin current $I_s(N_i, t)$ injected into the nonmagnetic metal N_i ($i = 1, 2, 3$) is calculated as

$$I_s(N_i, t) = - \sum_{\mathbf{q}, \mathbf{k}} \frac{4 \mathcal{J}_{sd}^{k-q} \sqrt{S_0}}{\sqrt{2N_F N_N} \hbar} \text{Re} C_{\mathbf{k}, \mathbf{q}}^<(t, t), \quad (\text{S1})$$

where N_F (N_N) is the number of lattice sites in F (N), S_0 is the size of the localized spins in F , and \mathcal{J}_{sd}^{k+q} is the Fourier transform of the s - d interaction at the F/N interface. Here, $C_{\mathbf{k}, \mathbf{q}}^<(t, t') = -i \langle a_{\mathbf{q}}^+(t') s_{\mathbf{k}}^-(t) \rangle$ measures the correlation between the magnon operator $a_{\mathbf{q}}^+$ and the spin-density operator $s_{\mathbf{k}}^- = (s_{\mathbf{k}}^x - i s_{\mathbf{k}}^y) / 2$. Note that the time dependence of $I_s(N_i, t)$ vanishes in the steady state and it is hereafter discarded. Introducing the frequency representation $C_{\mathbf{k}, \mathbf{q}}^<(t - t') = \int_{-\infty}^{\infty} \frac{d\omega}{2\pi} C_{\mathbf{k}, \mathbf{q}}^<(\omega) e^{-i\omega(t-t')}$ and adopting the representation [S2] $\check{C} = \begin{pmatrix} C^R & C^K \\ 0 & C^A \end{pmatrix}$ as well as using the relation $C^< = \frac{1}{2}[C^K - C^R + C^A]$, we obtain

$$I_s(N_1) = \sum_{\mathbf{q}, \mathbf{k}} \frac{-2 \mathcal{J}_{sd}^{k-q} \sqrt{S_0}}{\sqrt{2N_F N_N} \hbar} \int_{-\infty}^{\infty} \frac{d\omega}{2\pi} \text{Re} C_{\mathbf{k}, \mathbf{q}}^K(\omega) \quad (\text{S2})$$

for the spin current $I_s(N_1)$ in the steady state.

When we introduce a renormalized magnon propagator $\delta \check{X}_{\mathbf{q}}(\omega)$, the interface correlation \check{C} appearing in Eq. (S2) is generally expressed as

$$\check{C}_{\mathbf{k}, \mathbf{q}}(\omega) = \frac{\mathcal{J}_{sd}^{k-q} \sqrt{S_0}}{\sqrt{N_N N_F} \hbar} \check{\chi}_{\mathbf{k}}(\omega) \delta \check{X}_{\mathbf{q}}(\omega), \quad (\text{S3})$$

where $\check{\chi}_{\mathbf{k}}(\omega) = \begin{pmatrix} \chi_{\mathbf{k}}^R(\omega) & \chi_{\mathbf{k}}^K(\omega) \\ 0 & \chi_{\mathbf{k}}^A(\omega) \end{pmatrix}$ is the spin-density propagator satisfying the local equilibrium condition:

$$\chi_{\mathbf{k}}^A(\omega) = [\chi_{\mathbf{k}}^R(\omega)]^*; \quad \chi_{\mathbf{k}}^K(\omega) = 2i \text{Im} \chi_{\mathbf{k}}^R(\omega) \coth\left(\frac{\hbar\omega}{2k_B T}\right). \quad (\text{S4})$$

Here the retarded component of $\check{\chi}_{\mathbf{k}}(\omega)$ is given by $\chi_{\mathbf{k}}^R(\omega) = \chi_N / (1 + \lambda_{sf}^2 k^2 - i\omega\tau_{sf})$ [S3] where χ_N , λ_{sf} , and τ_{sf} are the paramagnetic susceptibility, the spin diffusion length, and spin relaxation time.

We now consider the phonon-dragged SSE [the process P_2 shown in FIG. 2 (b)]. The renormalized magnon propagator $\delta \check{X}_{\mathbf{q}}(\omega)$ in the present case is given by

$$\delta \check{X}_{\mathbf{q}}(\omega) = \check{X}_{\mathbf{q}}(\omega) \check{\Sigma}_{\mathbf{q}}(\omega) \check{X}_{\mathbf{q}}(\omega), \quad (\text{S5})$$

where $\check{X}_{\mathbf{q}}(\omega) = \begin{pmatrix} X_{\mathbf{q}}^R(\omega) & X_{\mathbf{q}}^K(\omega) \\ 0 & X_{\mathbf{q}}^A(\omega) \end{pmatrix}$ is the bare magnon propagator satisfying the equilibrium condition:

$$X_{\mathbf{q}}^A(\omega) = [X_{\mathbf{q}}^R(\omega)]^*; \quad X_{\mathbf{q}}^K(\omega) = 2i \text{Im} X_{\mathbf{q}}^R(\omega) \coth\left(\frac{\hbar\omega}{2k_B T}\right). \quad (\text{S6})$$

Here, the retarded component is given by $X_{\mathbf{q}}^R(\omega) = (\omega - \tilde{\omega}_{\mathbf{q}} + i\alpha\omega)^{-1}$, where $\tilde{\omega}_{\mathbf{q}} = \gamma H_0 + \omega_{\mathbf{q}}$ is the magnon frequency for uniform mode γH_0 and exchange mode

$\omega_{\mathbf{q}} = D_{\text{ex}}q^2/\hbar$. In Eq. (S5), the selfenergy $\check{\Sigma}$ due to phonons is given by

$$\check{\Sigma}_{\mathbf{q}}(\omega) = \frac{i}{2N_F} \sum_{\mathbf{K}} \left(\frac{\Gamma_{\mathbf{K},\mathbf{q}}}{\hbar} \right)^2 \int_{\nu} \left\{ \delta D^R(\nu) \check{X}_{\mathbf{q}_-}(\omega_-) \check{\tau}_1 + \delta D^A(\nu) \check{\tau}_1 \check{X}_{\mathbf{q}_-}(\omega_-) + \delta D^K(\nu) \check{X}_{\mathbf{q}_-}(\omega_-) \right\}, \quad (\text{S7})$$

where $\Gamma_{\mathbf{K},\mathbf{q}} = \tilde{g}\omega_{\mathbf{q}}\sqrt{\frac{\hbar\nu_{\mathbf{K}}}{2M_{\text{ion}}v_{\text{ph}}^2}}$ is the magnon-phonon interaction vertex with $\nu_{\mathbf{K}}$, v_{ph} and M_{ion} being the phonon frequency, phonon velocity and the ion mass, $\check{\tau}$ is the Pauli matrix in the Keldysh space, and we have introduced the shorthand notations $\omega_- = \omega - \nu$, $\mathbf{q}_- = \mathbf{q} - \mathbf{K}$, and $\int_{\nu} = \int_{-\infty}^{\infty} \frac{d\nu}{2\pi}$. In Eq. (S7), the full phonon propagator $\delta\hat{D}_{\mathbf{K}}$ [the whole of the phonon lines for P_2 in FIG. 2 (b)] is written as [S4]

$$\delta\hat{D}_{\mathbf{K}}(\nu) = \delta\hat{D}_{\mathbf{K}}^{l\text{-}eq}(\nu) + \delta\hat{D}_{\mathbf{K}}^{n\text{-}eq}(\nu). \quad (\text{S8})$$

Here, $\delta\hat{D}^{l\text{-}eq}(\omega) = \begin{pmatrix} \delta D^{l\text{-}eq,R}(\nu) & \delta D^{l\text{-}eq,K}(\nu) \\ 0 & \delta D^{l\text{-}eq,A}(\nu) \end{pmatrix}$ is the local-equilibrium propagator satisfying the local-equilibrium conditions $\delta D_{\mathbf{K}}^{l\text{-}eq,A}(\nu) = [\delta D_{\mathbf{K}}^{l\text{-}eq,R}(\nu)]^*$ and $\delta D_{\mathbf{K}}^{l\text{-}eq,K}(\nu) = [\delta D_{\mathbf{K}}^{l\text{-}eq,R}(\nu) - \delta D_{\mathbf{K}}^{l\text{-}eq,A}(\nu)] \coth(\frac{\hbar\nu}{2k_{\text{B}}T})$ with its retarded component given by

$$\delta D_{\mathbf{K}}^{l\text{-}eq,R}(\nu) = \frac{\Omega_0^2}{N_F(\Lambda/a_S)} \sum_{\mathbf{K}'} [D_{\mathbf{K}'}^R(\nu)]^2 D_{\mathbf{K}'}^R(\nu), \quad (\text{S9})$$

while $\delta\hat{D}^{n\text{-}eq} = \begin{pmatrix} 0 & \delta D^{n\text{-}eq,K} \\ 0 & 0 \end{pmatrix}$ is the nonequilibrium propagator with its Keldysh component given by

$$\delta D_{\mathbf{K}}^{n\text{-}eq,K}(\nu) = \frac{\Omega_0^2}{N_F(\Lambda/a_S)} \sum_{\mathbf{K}'} [D_{\mathbf{K}'}^R(\nu) - D_{\mathbf{K}'}^A(\nu)] |D_{\mathbf{K}'}^R(\nu)|^2 \times \left[\coth\left(\frac{\hbar\nu}{2k_{\text{B}}T_{F_2}}\right) - \coth\left(\frac{\hbar\nu}{2k_{\text{B}}T_{F_1}}\right) \right], \quad (\text{S10})$$

In the above equations, $\Omega_0 = \sqrt{K_{\text{ph}}/M_{\text{ion}}}$ with the elastic constant K_{ph} in F , and $\hat{D}_{\mathbf{K}}(\nu) = \begin{pmatrix} D_{\mathbf{K}}^R(\nu) & D_{\mathbf{K}}^K(\nu) \\ 0 & D_{\mathbf{K}}^A(\nu) \end{pmatrix}$ is

the bare phonon propagator satisfying the equilibrium condition:

$$D_{\mathbf{K}}^A(\nu) = [D_{\mathbf{K}}^R(\nu)]^*; \quad D_{\mathbf{K}}^K(\nu) = 2i \text{Im} D_{\mathbf{K}}^R(\nu) \coth\left(\frac{\hbar\nu}{2k_{\text{B}}T}\right), \quad (\text{S11})$$

with its retarded component and the phonon lifetime given by $D_{\mathbf{K}}^R(\nu) = (\nu - \nu_{\mathbf{K}} + i/\tau_{\text{ph}})^{-1} - (\nu + \nu_{\mathbf{K}} + i/\tau_{\text{ph}})^{-1}$ and τ_{ph} .

Now substituting these expressions into equation (S5) and use Eq. (S2), the spin current injected into N_1 by the phonon-drag process is calculated as

$$I_s^{\text{drag}}(N_1) = \frac{R}{N_N N_F} \sum_{\mathbf{k},\mathbf{q},\mathbf{K}} \int d\nu_{\mathbf{K}} \nu_{\mathbf{K}}^4 (\Gamma_{\mathbf{K},\mathbf{q}})^2 A_{\mathbf{k},\mathbf{q}}(\nu) \times \left[\coth\left(\frac{\hbar\nu_{\mathbf{K}}}{2k_{\text{B}}T_2}\right) - \coth\left(\frac{\hbar\nu_{\mathbf{K}}}{2k_{\text{B}}T_1}\right) \right], \quad (\text{S12})$$

where $R = \sqrt{2}(J_{sd}^2 S_0) \Omega_0^2 N_{\text{int}}(a_S/\Lambda) \tau_{\text{ph}} / (4\pi^3 \hbar^4 \nu_D^6)$ with $\nu_D = v_{\text{ph}}/a_S$, and

$$A_{\mathbf{k},\mathbf{q}}(\nu) = \int_{\omega} \text{Im} \chi_{\mathbf{k}}^R(\omega) \text{Im} X_{\mathbf{q}_-}^R(\omega_-) |X_{\mathbf{q}}^R(\omega)|^2 \times \left[\coth\left(\frac{\hbar\omega_-}{2k_{\text{B}}T_1}\right) - \coth\left(\frac{\hbar\omega}{2k_{\text{B}}T_1}\right) \right]. \quad (\text{S13})$$

By setting $T = T_2$, $\Delta T = T_1 - T_2$, $\Omega_0 = \nu_D$ and after some algebra, we obtain Eq. (3) in the main text.

References

- S1: H. Adachi, J. Ohe, S. Takahashi, and S. Maekawa, Phys. Rev. B (in press); arXiv:1010.2325.
- S2: A. I. Larkin and Yu. N. Ovchinnikov, Zh. Eksp. Teor. Fiz. **68**, 1915 (1975) [Sov. Phys. JETP **41**, 960 (1975)].
- S3: P. Fulde and A. Luther, Phys. Rev. **175**, 337 (1968).
- S4: K. Michaeli and A. M. Finkel'stein, Phys. Rev. B **80**, 115111 (2009).